Determination of $|V_{ub}|$ from Measurements of the Inclusive Charmless Semileptonic Partial Rates of B Mesons using Full Reconstruction Tags

I. Bizjak,[12] K. Abe,[7] K. Abe,[41] H. Aihara,[43] Y. Asano,[47] S. Bahinipati,[4] A. M. Bakich,[38] Y. Ban,[32] E. Barberio,[19] M. Barbero,[6] A. Bay,[16] U. Bitenc,[12] S. Blyth,[24] A. Bondar,[1] A. Bozek,[25] M. Bračko,[7,18,12] J. Brodzicka,[25] T. E. Browder,[6] Y. Chao,[24] A. Chen,[22] W. T. Chen,[22] B. G. Cheon,[3] R. Chistov,[11] S.-K. Choi,[5] Y. Choi,[37] Y. K. Choi,[37] A. Chuvikov,[33] S. Cole,[38] J. Dalseno,[19] M. Danilov,[11] M. Dash,[48] L. Y. Dong,[9] A. Drutskoy,[4] S. Eidelman,[1] Y. Enari,[20] F. Fang,[6] S. Fratina,[12] N. Gabyshev,[1] A. Garmash,[33] T. Gershon,[7] G. Gokhroo,[39] B. Golob,[17,12] A. Gorišek,[12] J. Haba,[7] T. Hara,[30] H. Hayashii,[21] M. Hazumi,[7] L. Hinz,[16] T. Hokuue,[20] Y. Hoshi,[41] S. Hou,[22] W.-S. Hou,[24] T. Iijima,[20] A. Imoto,[21] K. Inami,[20] A. Ishikawa,[7] R. Itoh,[7] M. Iwasaki,[43] Y. Iwasaki,[7] J. H. Kang,[49] J. S. Kang,[14] P. Kapusta,[25] N. Katayama,[7] H. Kawai,[2] T. Kawasaki,[27] H. R. Khan,[44] H. Kichimi,[7] H. J. Kim,[15] S. M. Kim,[37] K. Kinoshita,[4] S. Korpar,[18,12] P. Križan,[17,12] P. Krokovny,[1] R. Kulasiri,[4] S. Kumar,[31] C. C. Kuo,[22] A. Kuzmin,[1] Y.-J. Kwon,[49] G. Leder,[10] S. E. Lee,[36] T. Lesiak,[25] J. Li,[35] A. Limosani,[7] S.-W. Lin,[24] D. Liventsev,[11] J. MacNaughton,[10] G. Majumder,[39] F. Mandl,[10] T. Matsumoto,[45] A. Matyja,[25] Y. Mikami,[42] W. Mitaroff,[10] K. Miyabayashi,[21] H. Miyake,[30] H. Miyata,[27] R. Mizuk,[11] T. Nagamine,[42] Y. Nagasaka,[8] I. Nakamura,[7] E. Nakano,[29] M. Nakao,[7] Z. Natkaniec,[25] S. Nishida,[7] O. Nitoh,[46] T. Nozaki,[7] S. Ogawa,[40] T. Ohshima,[20] T. Okabe,[20] S. Okuno,[13] S. L. Olsen,[6] Y. Onuki,[27] W. Ostrowicz,[25] P. Pakhlov,[11] H. Park,[15] N. Parslow,[38] L. S. Peak,[38] R. Pestotnik,[12] L. E. Piilonen,[48] M. Rozanska,[25] H. Sagawa,[7] Y. Sakai,[7] N. Sato,[20] T. Schietinger,[16] O. Schneider,[16] P. Schönmeier,[42] C. Schwanda,[10] K. Senyo,[20] M. E. Sevior,[19] H. Shibuya,[40] B. Shwartz,[1] V. Sidorov,[1] A. Somov,[4] N. Soni,[31] R. Stamen,[7] S. Stanič,[28] M. Starič,[12] T. Sumiyoshi,[45] S. Suzuki,[34] S. Y. Suzuki,[7] O. Tajima,[7] F. Takasaki,[7] K. Tamai,[7] N. Tamura,[27] M. Tanaka,[7] Y. Teramoto,[29] X. C. Tian,[32] T. Tsuboyama,[7] T. Tsukamoto,[7] S. Uehara,[7] T. Uglov,[11] K. Ueno,[24] S. Uno,[7] P. Urquijo,[19] G. Varner,[6] K. E. Varvell,[38] S. Villa,[16] C. C. Wang,[24] C. H. Wang,[23] Y. Watanabe,[44] Q. L. Xie,[9] B. D. Yabsley,[48] A. Yamaguchi,[42] Y. Yamashita,[26] M. Yamauchi,[7] Heyoung Yang,[36] L. M. Zhang,[35] Z. P. Zhang,[35] V. Zhilich,[1] and D. Žontar[17,12]

(Belle Collaboration)

[1]*Budker Institute of Nuclear Physics, Novosibirsk*
[2]*Chiba University, Chiba*
[3]*Chonnam National University, Kwangju*
[4]*University of Cincinnati, Cincinnati, Ohio 45221*
[5]*Gyeongsang National University, Chinju*
[6]*University of Hawaii, Honolulu, Hawaii 96822*
[7]*High Energy Accelerator Research Organization (KEK), Tsukuba*
[8]*Hiroshima Institute of Technology, Hiroshima*
[9]*Institute of High Energy Physics, Chinese Academy of Sciences, Beijing*
[10]*Institute of High Energy Physics, Vienna*
[11]*Institute for Theoretical and Experimental Physics, Moscow*
[12]*J. Stefan Institute, Ljubljana*
[13]*Kanagawa University, Yokohama*
[14]*Korea University, Seoul*
[15]*Kyungpook National University, Taegu*
[16]*Swiss Federal Institute of Technology of Lausanne, EPFL, Lausanne*
[17]*University of Ljubljana, Ljubljana*
[18]*University of Maribor, Maribor*
[19]*University of Melbourne, Victoria*
[20]*Nagoya University, Nagoya*
[21]*Nara Women's University, Nara*
[22]*National Central University, Chung-li*
[23]*National United University, Miao Li*
[24]*Department of Physics, National Taiwan University, Taipei*
[25]*H. Niewodniczanski Institute of Nuclear Physics, Krakow*
[26]*Nippon Dental University, Niigata*
[27]*Niigata University, Niigata*
[28]*Nova Gorica Polytechnic, Nova Gorica*
[29]*Osaka City University, Osaka*

[30]*Osaka University, Osaka*
[31]*Panjab University, Chandigarh*
[32]*Peking University, Beijing*
[33]*Princeton University, Princeton, New Jersey 08544*
[34]*Saga University, Saga*
[35]*University of Science and Technology of China, Hefei*
[36]*Seoul National University, Seoul*
[37]*Sungkyunkwan University, Suwon*
[38]*University of Sydney, Sydney NSW*
[39]*Tata Institute of Fundamental Research, Bombay*
[40]*Toho University, Funabashi*
[41]*Tohoku Gakuin University, Tagajo*
[42]*Tohoku University, Sendai*
[43]*Department of Physics, University of Tokyo, Tokyo*
[44]*Tokyo Institute of Technology, Tokyo*
[45]*Tokyo Metropolitan University, Tokyo*
[46]*Tokyo University of Agriculture and Technology, Tokyo*
[47]*University of Tsukuba, Tsukuba*
[48]*Virginia Polytechnic Institute and State University, Blacksburg, Virginia 24061*
[49]*Yonsei University, Seoul*
(Received 27 May 2005; published 8 December 2005)

We present a measurement of the Cabibbo-Kobayashi-Maskawa matrix element $|V_{ub}|$, based on 253 fb^{-1} of data collected by the Belle detector at the KEKB e^+e^- asymmetric collider. Events are tagged by fully reconstructing one of the B mesons, produced in pairs from $\Upsilon(4S)$. The signal for $b \to u$ semileptonic decay is distinguished from the $b \to c$ background using the hadronic mass M_X, the leptonic invariant mass squared q^2 and the variable $P_+ \equiv E_X - |\vec{p}_X|$. The results are obtained for events with $p_\ell^* \geq 1$ GeV$/c$, in three kinematic regions (1) $M_X < 1.7$ GeV$/c^2$, (2) $M_X < 1.7$ GeV$/c^2$ combined with $q^2 > 8$ GeV$^2/c^2$, and by (3) $P_+ < 0.66$ GeV$/c$. The matrix element $|V_{ub}|$ is found to be $(4.09 \pm 0.19 \pm 0.20^{+0.14}_{-0.15} \pm 0.18) \times 10^{-3}$, where the errors are statistical, systematic including Monte Carlo modeling, theoretical, and from shape function parameter determination, respectively.

DOI: 10.1103/PhysRevLett.95.241801 PACS numbers: 12.15.Hh, 11.30.Er, 13.25.Hw

An accurate knowledge of the Cabibbo-Kobayashi-Maskawa matrix element $|V_{ub}|$ is crucial to test standard model predictions for CP violation. Currently, the best precision may be achieved by measuring the inclusive rate $\Delta\Gamma_{u\ell\nu}(\Delta\Phi)$ of $B \to X_u \ell\nu$ decays in a restricted region of the phase space $(\Delta\Phi)$ where the dominant charm background is suppressed and theoretical uncertainties are minimized. The theoretical factor $R(\Delta\Phi)$ directly relates the inclusive rate to $|V_{ub}|$, with no extrapolation to the full phase space: $|V_{ub}|^2 = \Delta\Gamma_{u\ell\nu}(\Delta\Phi)/R(\Delta\Phi)$. Here we report measurements of $\Delta\Gamma_{u\ell\nu}(\Delta\Phi)$ for several choices of $\Delta\Phi$ and derive the corresponding values of $|V_{ub}|$.

The measurements are made with a sample of events where the hadronic decay mode of the tagging side B meson, B_{tag}, is fully reconstructed, while the semileptonic decay of the signal side B meson, B_{sig}, is identified by the presence of a high momentum electron or muon. B denotes both charged and neutral B mesons. This method allows the construction of the invariant masses of the hadronic (M_X) and leptonic $(\sqrt{q^2})$ system in the semileptonic decay, and the variable $P_+ \equiv E_X - |\vec{p}_X|$, where E_X is the energy and $|\vec{p}_X|$ the magnitude of the three-momentum of the hadronic system. These inclusive kinematic variables can be used to separate the $B \to X_u \ell\nu$ decays from the much more abundant $B \to X_c \ell\nu$ decays. Three competing kinematic regions $(\Delta\Phi)$ were proposed by theoretical studies [1,2], based on the three kinematic variables, and are directly compared by this analysis. The value of $|V_{ub}|$ is extracted using recent theoretical calculations [2,3] that include all the currently known contributions. M_X and q^2 selections were already used to extract $|V_{ub}|$ [4,5]. The present analysis is the first one to use P_+ and to directly compare the three methods.

The data were collected with the Belle detector [6] at the asymmetric-energy KEKB storage ring [7]. The results presented in this Letter are based on a 253 fb^{-1} sample recorded at the $\Upsilon(4S)$ resonance, which contains $275 \times 10^6 B\overline{B}$ pairs. An additional 28 fb^{-1} sample taken at a center-of-mass energy 60 MeV below the $\Upsilon(4S)$ resonance is used to subtract the background from $e^+e^- \to q\bar{q}$ $(q = u, d, s, c)$.

Monte Carlo (MC) simulated events were used to determine efficiencies as well as signal and background distributions. The detector simulation was based on GEANT [8]. To model $B \to X_u \ell\nu$ we use the EVTGEN generator [9] with various models, where X_u is π or ρ [10], an excited X_u state [11], or a nonresonant multiparticle final state [12]. The $B \to X_c \ell\nu$ transitions are simulated according to the

QQ generator [13]. For the two dominant contributions, $D^* \ell \nu$ and $D \ell \nu$, we use a HQET-based parametrization of form factors [14] and ISGW2 model [11], respectively. For the D^{**} we use ISGW2 model and for subcomponents D_1 and D_2^* set $\frac{\mathcal{B} \to D_1 \ell \nu + \mathcal{B} \to D_2^* \ell \nu}{\mathcal{B} \to D^{**} \ell \nu} = 0.35 \pm 0.23$. The motion of the b quark inside the B meson is implemented with the introduction of a shape function [12,15] that describes the b quark momentum distribution inside the B meson.

The $B_{\rm tag}$ candidates are reconstructed in the modes $B \to D^{(*)}\pi/\rho/a_1/D_s^{(*)}$, $\overline{D}^0 \to K^+\pi^-$, $K^+\pi^-\pi^0$, $K^+\pi^+\pi^-\pi^-$, $K_S^0\pi^0$, $K_S^0\pi^+\pi^-$, $K_S^0\pi^+\pi^-\pi^0$, and K^+K^-, $D^- \to K^+\pi^-\pi^-$, $K^+\pi^-\pi^-\pi^0$, $K_S^0\pi^-$, $K_S^0\pi^-\pi^0$, $K_S^0\pi^-\pi^-\pi^+$, and $K^+K^-\pi^-$, and $D_s^+ \to K_S^0 K^+$ and $K^+K^-\pi^+$. $\overline{D}^*$ mesons are reconstructed by combining a $\overline{D}$ candidate and a soft pion or photon. (Inclusion of charge conjugate decays is implied throughout this Letter.) The selection of $B_{\rm tag}$ candidates is based on the beam-constrained mass, $M_{\rm bc} = \sqrt{E_{\rm beam}^{*2}/c^4 - p_B^{*2}/c^2}$, and the energy difference, $\Delta E = E_B^* - E_{\rm beam}^*$. Here $E_{\rm beam}^* = \sqrt{s}/2 \simeq 5.290$ GeV is the beam energy in the e^+e^- center-of-mass system (cms), and p_B^* and E_B^* are the cms momentum and energy of the reconstructed B meson. (Throughout this Letter the variables calculated in the cms are denoted with an asterisk.)

The combinatorial background from jetlike $e^+e^- \to q\bar{q}$ processes is suppressed by an event topology requirement based on the normalized second Fox-Wolfram moment $R_2 < 0.5$ [16], and for some modes also by $|\cos\theta_{\rm thrust}^*| < 0.8$, where $\theta_{\rm thrust}^*$ is the angle between the thrust axis of the $B_{\rm tag}$ candidate and that of the rest of the event. To minimize the fraction of events with incorrect separation of tag and signal sides while maintaining high signal efficiency, a loose selection requirement of $M_{\rm bc} \geq 5.22$ GeV$/c^2$ and $-0.2 < \Delta E < 0.05$ GeV is made. If an event has multiple $B_{\rm tag}$ candidates, we choose the one having the smallest χ^2 based on ΔE, the D candidate mass, and the $D^* - D$ mass difference if applicable.

For events tagged by fully reconstructed $B_{\rm tag}$ candidates, we search for electrons or muons from semileptonic decays of $B_{\rm sig}$. We require a lepton with momentum p_ℓ^* exceeding 1 GeV$/c$ in the laboratory polar angular region of $26° \leq \theta \leq 140°$. Leptons from J/ψ decay, photon conversion in the material of the detector, and π^0 decay are rejected based on the invariant mass they form in combination with an oppositely charged lepton and for electron candidates also with an additional photon. When the $B_{\rm tag}$ candidate is charged, we also require the lepton charge to be consistent with that from prompt semileptonic decay. The signal yield is obtained by fitting the $M_{\rm bc}$ distribution to the sum of an empirical parametrization of the combinatorial background shape [17] plus a signal shape [18] that peaks at the B mass and taking the part of the signal that lies in the "signal region," $M_{\rm bc} \geq 5.27$ GeV$/c^2$, as shown in Fig. 1(a). The cutoff for $M_{\rm bc}$ reduces the uncertainty

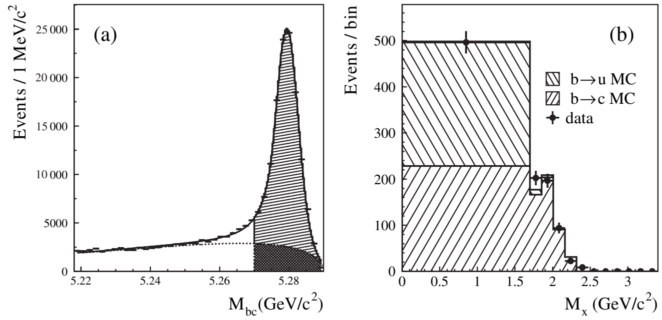

FIG. 1. (a) Distribution in $M_{\rm bc}$ (data) of $B_{\rm tag}$ candidates in events satisfying $B_{\rm sig}$ selection. (b) M_X distribution for events with $q^2 > 8$ GeV$^2/c^2$, with fitted contributions of $B \to X_c \ell \nu$ and $B \to X_u \ell \nu$.

from the incorrect assignment of tag and signal sides in signal events.

The $B \to X_u \ell \nu$ signal events are selected by removing poorly measured soft charged tracks and imposing several additional requirements to reject poorly reconstructed events and suppress the $B \to X_c \ell \nu$ background. We require that the event contain exactly one lepton and have zero net charge and that the invariant mass squared of the missing four-momentum $m_{\rm miss}^2 \equiv (p_{\Upsilon(4S)} - p_{B_{\rm tag}} - p_X - p_\ell)^2$ [$p_{\Upsilon(4S)}$, $p_{B_{\rm tag}}$, and p_X are four-momenta of the $\Upsilon(4S)$, $B_{\rm tag}$, and hadronic system (X), respectively] be within $-1 \leq m_{\rm miss}^2 \leq 0.5$ GeV$^2/c^4$. To suppress the $B \to X_c \ell \nu$ background, events with a $K^\pm$ or K_S^0 candidate on the signal side are rejected (kaon veto). To reject events containing a K_L^0, we require that the angle between the missing momentum and the direction of any K_L^0 candidate, reconstructed in the K_L^0 detector, be greater than 37°. We also reject $B^0 \to D^{*+}\ell^-\bar{\nu}$ events by detecting the slow pion (π_s) from $D^{*+} \to D^0\pi_s^+$ and deducing from its momentum the momentum of the D^{*+}. The missing mass squared $m_{\rm miss(D^*)}^2 = (p_B - p_{D^*} - p_\ell)^2$ is calculated from the reconstructed quantities, and events with $m_{\rm miss(D^*)}^2 > -3$ GeV$^2/c^4$ are rejected.

Finally, the kinematic variables M_X and P_+ are calculated from the measured momenta of all charged tracks and energy deposits of all neutral clusters in the electromagnetic calorimeter that are not used in the $B_{\rm tag}$ reconstruction or for the lepton candidate. The four-momentum of the leptonic system is calculated as $q = p_{\Upsilon(4S)} - p_{B_{\rm tag}} - p_X$. The distributions of events in M_X and P_+ are obtained by fitting the $M_{\rm bc}$ distribution, as described above, in bins of M_X and P_+. Figs. 1(b), 2(a), and 3(a) show the resulting M_X and P_+ distributions. We define three kinematic signal regions ($\Delta\Phi$) for events where the prompt lepton has $p_\ell^* \geq 1$ GeV$/c$: $P_+ < 0.66$ GeV$/c$, $M_X < 1.7$ GeV$/c^2$, and $M_X < 1.7$ GeV$/c^2$ combined with $q^2 > 8$ GeV$^2/c^2$. These three regions are denoted as P_+, M_X, and M_X/q^2, respectively. To minimize the systematic effects of uncertainties in lepton selection and full reconstruction, we

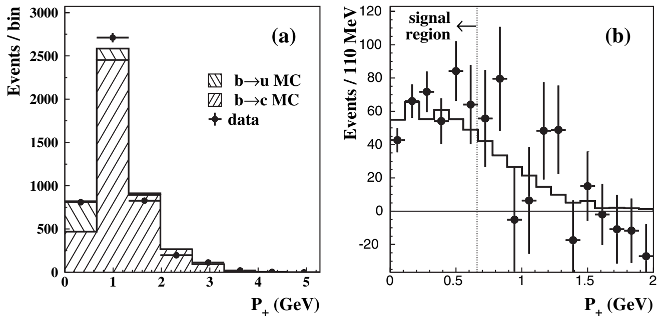

FIG. 2. (a) The P_+ distribution for the selected events, with fitted contributions from $B \to X_c \ell \nu$ and $B \to X_u \ell \nu$, (b) P_+ distribution (symbols with error bars) after subtracting $B \to X_c \ell \nu$, with fitted $B \to X_u \ell \nu$ contribution (histogram).

normalize the partial rate for each signal region with the total semileptonic rate:

$$W = \frac{\Delta\Gamma_{u\ell\nu}(\Delta\Phi)}{\Gamma(X\ell\nu)} = \frac{N^{\rm raw}_{b\to u}}{N_{\rm sl}} \times \frac{F}{\varepsilon^{b\to u}_{\rm sel}} \times \frac{\varepsilon^{\rm sl}_{\rm frec}}{\varepsilon^{b\to u}_{\rm frec}} \times \frac{\varepsilon^{\rm sl}_{\ell}}{\varepsilon^{b\to u}_{\ell}}. \quad (1)$$

To extract the raw number of signal events, $N^{\rm raw}_{b\to u}$, we fit the M_X and P_+ distributions with MC-determined shapes for $B \to X_u \ell \nu$ and $B \to X_c \ell \nu$ and subtract the $B \to X_c \ell \nu$ contribution. The results for the M_X/q^2 and P_+ regions are shown in Figs. 1(b) and 2(a), respectively. MC simulation is used to estimate the conversion factor F of the observed number of events $N^{\rm raw}_{b\to u}$ to the number of signal events produced in the region in question and observed anywhere, and to estimate the efficiency for these events, $\varepsilon^{b\to u}_{\rm sel}$.

$N_{\rm sl} = (9.14 \pm 0.05) \times 10^4$ is the number of events having at least one lepton with $p^*_\ell \geq 1$ GeV$/c$, determined from a fit to the corresponding $M_{\rm bc}$ distribution [Fig. 1(a)], and corrected for the expected fraction of background events from nonsemileptonic decays (14.0%), as estimated by MC simulation. The factor $\varepsilon^{\rm sl}_{\rm frec}/\varepsilon^{b\to u}_{\rm frec}$ accounts for a possible difference in the $B_{\rm tag}$ reconstruction efficiency in the presence of a semileptonic or $B \to X_u \ell \nu$ decay; $\varepsilon^{\rm sl}_{\ell}/\varepsilon^{b\to u}_{\ell}$ is the ratio of both lepton identification efficiencies and fractions of semileptonic decay leptons with $p^*_\ell \geq 1$ GeV$/c$, in the whole kinematic phase space for semileptonic decays, and within the kinematic signal region for signal events. The product of efficiency ratios $r^{\rm sl}_{b\to u} \equiv \varepsilon^{\rm sl}_{\rm frec}/\varepsilon^{b\to u}_{\rm frec} \times \varepsilon^{\rm sl}_{\ell}/\varepsilon^{b\to u}_{\ell}$ is obtained from MC simulation. Table I summarizes the results for $N^{\rm raw}_{b\to u}$, $\varepsilon^{b\to u}_{\rm sel}$, F, and $r^{\rm sl}_{b\to u}$ for all three signal regions, where the error in $N^{\rm raw}_{b\to u}$ is statistical only. Inserting these values in Eq. (1), we obtain the three values of W. As both numerator and denominator of W have been obtained from the same tag sample, the B^0/B^+ weightings are the same, and W has no dependence on lifetimes. Multiplying W by the average measured semileptonic rate $\Gamma(X\ell\nu) = \mathcal{B}(B \to X\ell\nu)/\tau_B$, obtained from $\mathcal{B}(B \to X\ell\nu) = 0.1073 \pm 0.0028$ and $\tau_B = (1.604 \pm 0.016)$ ps [19], gives the average $\Delta\Gamma_{u\ell\nu}(\Delta\Phi)$. The results with relative errors are given in Table II.

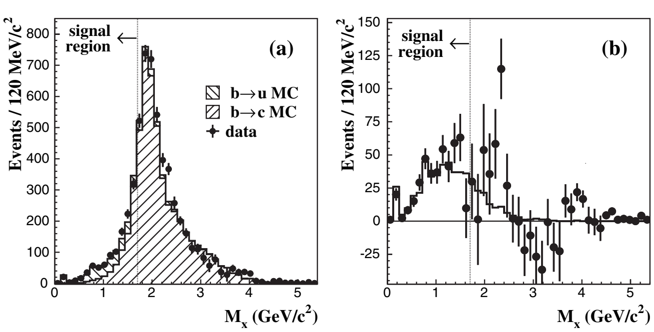

FIG. 3. M_X distribution (no q^2 requirement) with fitted contributions from $X_c \ell \nu$ and $X_u \ell \nu$: (a) before and (b) after subtracting the $X_c \ell \nu$ contribution (symbols with error bars), shown with the prediction for $X_c \ell \nu$ (MC, histogram).

We divide the experimental error into four categories: statistical, systematic, $b \to c$, and $b \to u$ MC modeling errors, and summarize them in Table II for the three $\Delta\Gamma_{u\ell\nu}(\Delta\Phi)$ measurements. The two modeling errors include the uncertainty in signal event extraction, efficiency and unfolding factor determination due to the choice of specific theoretical models, and values of the parameters used in our MC predictions. For signal $B \to X_u \ell \nu$ MC, the shape function parameters $\Lambda^{\rm SF} = (0.66 \pm 0.15)$ GeV$/c^2$ and $\lambda_1^{\rm SF} = -(0.40 \pm 0.20)$ GeV$^2/c^2$ were varied within the stated limits, taking into account the negative correlation between them [20]. To take into account the uncertainty of the prediction in Ref. [12], we use a factor of 2 larger error for $\Lambda^{\rm SF}$ than was determined in Ref. [20]. For $B \to X_c \ell \nu$ MC, the uncertainty due to our limited knowledge of branching fractions is studied by varying the contributions of $D\ell\nu$ and $D^*\ell\nu$ and the relative fraction of narrow states D_1 and D_2^* that contribute to $D^{**}\ell\nu$ to estimate the modeling error of the D^{**} region. The uncertainty from form factor modeling in $D\ell\nu$ and $D^*\ell\nu$ was studied by varying the parameters $\rho_D^2 = 1.15 \pm 0.16$ and $\rho_A^2 = 1.56 \pm 0.13$ within their errors [19]. The validity of the $B \to X_c \ell \nu$ simulation was tested on a $B \to X_c \ell \nu$ enhanced control sample, where all selection requirements are applied but with the kaon veto reversed. The kinematic distributions of this control sample are accurately described by the simulation. Other sources of uncertainties, namely, limited MC statistics, extraction of $r^{\rm sl}_{b\to u}$, fitting procedure, and imperfect detector simulation are combined

TABLE I. $N^{\rm raw}_{b\to u}$, $\varepsilon^{b\to u}_{\rm sel}$, F, and $r^{\rm sl}_{b\to u}$ for the three kinematic signal regions.

$\Delta\Phi$	$N^{\rm raw}_{b\to u}$	$\varepsilon^{b\to u}_{\rm sel}$	F	$r^{\rm sl}_{b\to u}$
M_X/q^2	268 ± 27	26.5%	1.03	0.687 ± 0.014
M_X	404 ± 37	28.7%	1.07	0.700 ± 0.011
P_+	340 ± 32	25.5%	1.01	0.700 ± 0.012

TABLE II. Partial rates to the three kinematic signal regions with relative errors (in %).

$\Delta\Phi$	$\Delta\Gamma_{u\ell\nu}(\Delta\Phi)$	Stat	Syst	$b \to u$	$b \to c$
M_X/q^2	5.24×10^{-4} ps^{-1}	10.0	8.9	6.2	5.3
M_X	7.71×10^{-4} ps^{-1}	9.1	7.1	6.1	2.2
P_+	6.89×10^{-4} ps^{-1}	9.4	9.3	6.4	8.7

in the systematic error. The uncertainties due to inaccurate simulation of tracking, particle identification, and cluster finding are estimated by varying for each source the efficiency within the expected error and taking the maximum change in $\Delta\Gamma_{u\ell\nu}(\Delta\Phi)$ as the error. For each of these sources the effects on simulated $b \to u$ and $b \to c$ events are correlated, and the associated shifts are summed linearly. The net contributions from the three sources are then summed in quadrature.

The CKM matrix element $|V_{ub}|$ is obtained directly from the partial rate using $|V_{ub}|^2 = \Delta\Gamma_{u\ell\nu}(\Delta\Phi)/R(\Delta\Phi)$. $R(\Delta\Phi)$ is the theoretical prediction of $\Delta\Gamma_{u\ell\nu}(\Delta\Phi)$, the partial rate with a prompt lepton with $p_\ell^* \geq 1$ GeV$/c$, divided by $|V_{ub}|^2$. The values of R (in ps^{-1}) are calculated to be $23.7 \pm 2.0(\mathrm{SF})^{+2.5}_{-2.3}(\mathrm{th})$, $46.1 \pm 4.2(\mathrm{SF})^{+3.5}_{-3.2}(\mathrm{th})$, and $39.4 \pm 4.5(\mathrm{SF})^{+2.8}_{-2.7}(\mathrm{th})$ for the M_X/q^2, M_X, and P_+ signal regions, respectively. The $R(\Delta\Phi)$ values and their errors (SF) are calculated using the shape function scheme [15] parameters $m_b(\mathrm{SF}) = (4.60 \pm 0.04)$ GeV$/c^2$ and $\mu_\pi^2(\mathrm{SF}) = (0.20 \pm 0.04)$ GeV$^2/c^2$ with correlation coefficient $\rho = -0.26$, obtained from the result of a global fit to moments of both $b \to c\ell\nu$ and $b \to s\gamma$ distributions [21]. While the dependence of $R(\Delta\Phi)$ on $\mu_\pi^2(\mathrm{SF})$ is small, we can approximate the dependence on $m_b(\mathrm{SF})$ as $R/R(m_b^0) - 1 = k(\Delta\Phi)(m_b/m_b^0 - 1)$, where $m_b^0 = 4.60$ GeV$/c^2$ and $k(\Delta\Phi)$ is found to be 2.09, 2.29, and 3.00 for the M_X/q^2, M_X, and P_+ signal regions, respectively. The theoretical error of R (th) is estimated by varying the subleading shape functions (four models), the matching scales μ_h, μ_i, $\bar{\mu}$, and weak annihilation [15]. The values of $|V_{ub}|$ with errors are given in Table III. The total error on $|V_{ub}|$ is 10%, 9%, and 11% for M_X/q^2, M_X, and P_+ regions, respectively. When the shape function parameters and R are better determined, $|V_{ub}|$ can be recalculated from $\Delta\Gamma_{u\ell\nu}(\Delta\Phi)$ shown in Table II.

The precision of the $|V_{ub}|$ determination is better than previous measurements [4,5,22], owing to the use of larger data sample, better shape function parameter determination, and improved theoretical predictions [2,3]. We find that the usage of the variable P_+ is more sensitive to $b \to c$ modeling and shape function parametrization than the other two methods and will become competitive in the future when the theoretical error of R dominates. No significant experimental nor theoretical improvement was observed by applying the additional selection $q^2 > 8$ GeV$^2/c^2$ to the M_X analysis. Taking correlations into account, we find that the difference between $|V_{ub}|$ values for M_X/q^2 and M_X regions has a significance of 2.7σ. We conclude that the results are consistent within errors, but we do not rule out possible effects of duality violation or weak annihilation contribution. We chose the M_X signal region result for our $|V_{ub}|$ determination, since it includes the largest portion of phase space and is least affected by the uncertainties: $|V_{ub}| = (4.09 \pm 0.19 \pm 0.20^{+0.14}_{-0.15} \pm 0.18) \times 10^{-3}$, where the errors are statistical, systematic with MC modeling, theoretical, and from shape function parameter determination, respectively. The effectiveness of $|V_{ub}|$ measurements using full reconstruction tagging is clear [Figs. 2(b) and 3(b)].

TABLE III. Values for $|V_{ub}|$ with relative errors (in %) for the three kinematic signal regions. Shape function parameters used in the calculation are $m_b(\mathrm{SF}) = (4.60 \pm 0.04)$ GeV$/c^2$ and $\mu_\pi^2(\mathrm{SF}) = (0.20 \pm 0.04)$ GeV$^2/c^2$.

$\Delta\Phi$	$\lvert V_{ub}\rvert \times 10^3$	Stat	Syst	$b \to u$	$b \to c$	SF	th
M_X/q^2	4.70	5.0	4.4	3.1	2.7	4.2	$^{+4.8}_{-5.2}$
M_X	4.09	4.6	3.5	3.1	1.1	4.5	$^{+3.5}_{-3.8}$
P_+	4.19	4.7	4.6	3.2	4.4	5.8	$^{+3.4}_{-3.5}$

We thank the KEKB group for excellent accelerator operations, the KEK cryogenics group for efficient operation of the solenoid, and the KEK computer group and NII for valuable computing and Super-SINET network support. We acknowledge support from MEXT and JSPS (Japan); ARC and DEST (Australia); NSFC (Contract No. 10175071, China); DST (India); the BK21 program of MOEHRD and the CHEP SRC program of KOSEF (Korea); KBN (Contract No. 2P03B 01324, Poland); MIST (Russia); MHEST (Slovenia); SNSF (Switzerland); NSC and MOE (Taiwan); and DOE (USA). We are grateful to B. Lange, M. Neubert, and G. Paz for providing us with their theoretical computations implemented in an inclusive generator. We would specially like to thank M. Neubert for valuable discussions and suggestions.

[1] C. W. Bauer, Z. Ligeti, and M. Luke, Phys. Rev. D **64**, 113004 (2001).

[2] S. W. Bosch, B. O. Lange, M. Neubert, and G. Paz, Phys. Rev. Lett. **93**, 221801 (2004); Nucl. Phys. **B699**, 335 (2004).

[3] M. Neubert, Eur. Phys. J. C **40**, 165 (2005); Phys. Lett. B **612**, 13 (2005); S. W. Bosch, M. Neubert, and G. Paz, J. High Energy Phys. 11 (2004) 073.

[4] B. Aubert *et al.* (*BABAR* Collaboration), Phys. Rev. Lett. **92**, 071802 (2004).

[5] H. Kakuno *et al.* (Belle Collaboration), Phys. Rev. Lett. **92**, 101801 (2004).

[6] A. Abashian *et al.* (Belle Collaboration), Nucl. Instrum. Methods Phys. Res., Sect. A **479**, 117 (2002).

[7] S. Kurokawa and E. Kikutani, Nucl. Instrum. Methods Phys. Res., Sect. A **499**, 1 (2003), and other papers in this volume.

[8] R. Brun, F. Bruyant, M. Maire, A. C. McPherson, and P. Zanarini, CERN Report No. DD/EE/84-1 (1984).

[9] D. J. Lange, Nucl. Instrum. Methods Phys. Res., Sect. A **462**, 152 (2001).

[10] P. Ball, hep-ph/0306251.

[11] D. Scora and N. Isgur, Phys. Rev. D **52**, 2783 (1995).

[12] F. De Fazio and M. Neubert, J. High Energy Phys. 06 (1999) 017.

[13] QQ event generator, developed by CLEO Collaboration, see http://www.lns.cornell.edu/public/CLEO/soft/QQ.

[14] M. Neubert, Phys. Rep. **245**, 259 (1994).

[15] B. O. Lange, M. Neubert, and G. Paz, Phys. Rev. D **72**, 073006 (2005).

[16] G. C. Fox and S. Wolfram, Phys. Rev. Lett. **41**, 1581 (1978).

[17] H. Albrecht *et al.* (ARGUS Collaboration), Z. Phys. C **48**, 543 (1990).

[18] J. E. Gaiser *et al.*, Phys. Rev. D **34**, 711 (1986).

[19] S. Eidelman *et al.*, Phys. Lett. B **592**, 1 (2004).

[20] A. Limosani and T. Nozaki (Heavy Flavor Averaging Group), hep-ex/0407052.

[21] O. Buchmueller and H. Flaecher (Heavy Flavor Averaging Group), hep-ph/0507253.

[22] R. Barate *et al.* (ALEPH Collaboration), Eur. Phys. J. C **6**, 555 (1999); M. Acciarri *et al.* (L3 Collaboration), Phys. Lett. B **436**, 174 (1998); P. Abreu *et al.* (DELPHI Collaboration), Phys. Lett. B **478**, 14 (2000); G. Abbiendi *et al.* (OPAL Collaboration), Eur. Phys. J. C **21**, 399 (2001); A. Bornheim *et al.* (CLEO Collaboration), Phys. Rev. Lett. **88**, 231803 (2002).